Adsorption (2013) 19:1035–1043
DOI 10.1007/s10450-013-9524-5

Adsorption of benzene and ethanol on activated carbon nanofibers prepared by electrospinning

**Yu Bai · Zheng-Hong Huang · Ming-Xi Wang ·
Feiyu Kang**

Received: 17 October 2012 / Accepted: 18 February 2013 / Published online: 3 March 2013

Abstract Activated carbon nanofibers (ACNFs) were prepared by electrospinning polyacrylonitrile solutions, and subsequent steam activation process. The ACNFs were characterized by scanning electron microscope, X-ray photoelectron spectroscopy and nitrogen adsorption at 77 K. The adsorption equilibrium data for benzene and ethanol were obtained by using static vapor adsorption system. As-prepared ACNFs demonstrate higher adsorption capacities for volatile organic compounds (VOCs) than activated carbon fibers (ACFs) by virtue of smaller diameter and more available adsorption sites on the surface. The adsorption performance of ACNFs increases with the burn-off, as a result of the increased microporosity. In addition, it is noteworthy that surface chemistry has an important effect on the adsorption of polar VOCs. The ACNF with higher oxygen content has a stronger adsorption tendency for ethanol.

Keywords Adsorption · Activated carbon nanofibers (ACNFs) · VOCs · Microporosity · Surface chemistry

1 Introduction

It has been well known that volatile organic compounds (VOCs) are harmful to both human beings and our living environment. As an effective technique to remove low-concentration VOCs, adsorption techniques have attracted more and more interests in recent years (Dwivedi et al. 2004; Lillo-Ródenas et al. 2005; Ramos et al. 2010). Usually, porous carbon materials, such as activated carbons (ACs) and activated carbon fibers (ACFs) are common adsorbents which are widely studied (Benkhedda et al. 2000; Dolidovich et al. 1999; Yi et al. 2009; Dwivedi et al. 2004). Recently, activated carbon nanofibers (ACNFs) have showed great potential in the removal of VOCs due to their smaller diameter (sub-micrometer) and more developed micropore compared with ACFs (Ramos et al. 2010; Shim et al. 2006; Oh et al. 2008a, b; Cuervo et al. 2008; Hsieh and Chou 2006; Lee et al. 2010); Tavanai et al. (2009) found that the microporosity of ACNFs was more developed than that of ACFs. In spite of lower specific surface area, carbon nanofibers have shown higher adsorption amounts for benzene and toluene, compared to ACs (Jahangiri et al. 2011). In this context, ACNFs can be novel and effective adsorbent for VOCs.

Though the surface structure and the adsorption performance for VOCs of ACNFs have been studied, few data about the difference between ACNFs and ACFs in the adsorption performance for VOCs has been reported so far. It is very important to compare the adsorption performance of ACNFs with that of ACFs, through which the better adsorption characteristics of ACNFs can be observed clearly to highlight the effectiveness of ACNFs as novel adsorbent material, especially when ACNFs and ACFs have similar porosity.

In the aspect of factors affecting the adsorption properties of ACNFs for VOCs, it must be emphasized that the adsorption process involves the interaction between adsorbent and adsorbate. For VOC with specific polarity, both the porous structure and the surface chemistry play important roles. Most researchers mainly focus on the characterization of common textual parameters of ACNFs

---

Y. Bai · Z.-H. Huang (✉) · M.-X. Wang · F. Kang (✉)
Lab of Advanced Materials, School of Materials Science and Engineering, Tsinghua University, 100084 Beijing, China
e-mail: zhhuang@mail.tsinghua.edu.cn

F. Kang
e-mail: fykang@tsinghua.edu.cn

without analyzing the effect of surface chemistry. In addition, considering that different VOC molecules have different properties, such as molecule structure and polarity, the adsorption performance of ACNFs may also be affected by the properties of different VOCs (Tsai et al. 2008; Chen et al. 2007). However, most VOCs adsorbed on the ACNFs in literature were molecules with similar properties.

The present work reports the adsorption equilibrium isotherms of benzene and ethanol (2 VOC molecules with different structure and polarity) on ACNFs prepared by electrospinning and subsequent activation process with steam. Comparing with ACFs, the superior adsorption performance of ACNFs with smaller fiber diameter was verified. Furthermore, the porosity and surface characteristics of ACNFs prepared by different activation conditions were characterized. Combining the characteristics of ACNFs with those of different VOC molecules, we studied the adsorption performance of ACNFs for benzene and ethanol. These results will be very helpful for understanding the adsorption mechanism of VOCs on ACNFs and developing the ACNFs with better adsorption properties for specific VOC molecule.

2 Experimental

2.1 Preparation of ACNFs and ACF

Polyacrylonitrile (PAN) (ONTARIO, New York, USA) was dissolved in N,N-dimethylformamide (DMF) (Beijing Modern Eastern Finechemical Co., Ltd, China) with concentrations of 10 and 15 wt% to form polymer solutions. The detailed electrospinning process was described in our previous work (Wang et al. 2011a, b). Stabilization of the electrospun fibers was carried out by heating the samples to 280 °C at a rate of 1 °C min^{-1} in air and kept at 280 °C for 2 h. Then the fibers were further heated up and carbonized at 800 or 850 °C for 30 min in nitrogen with a flow rate of 212 mL min^{-1} controlled by the rotameter. The samples were then activated by adding 30 vol.% steam controlled by the peristaltic pump into nitrogen flow at the same temperature for 10, 30 and 50 min. The weights of the stabilized electrospun fibers and the resultant samples were measured to calculate the burn-offs (The burn-off is defined as the fraction of the lost weight of the derived sample relative to the stabilized electrospun fiber). For comparison, activated carbon fibers (ACFs) were prepared from oxidized PAN fibers (Jilin Carbon Plant, China) by carbonization at 850 °C for 30 min and then activated at the same temperature with nitrogen flow containing 50 vol.% steam for 30 min.

The conditions for carbonization and activation for electrospun PAN nanofibers and meltspun fibers are summarized in (Table 1), with sample IDs used in the present work. Since the diameters of the electrospun PAN fibers are much smaller than those of meltspun fibers, the resultant activated carbon fibers prepared from the formers are called ACNFs, and the meltspun ones are named as ACFs.

2.2 Characterization

The surface morphology of samples was observed by the scanning electron microscope (SEM, LEO-1,530, Germany). The textural properties were investigated from the N_2 adsorption/desorption isotherm at 77 K (Belsorp-max, BEL, Japan). Before the measurements, samples were degassed at 200 °C for ~10 h. Total specific surface area (S_T), micropore volume (V_m) and average pore width (APW) were evaluated by the t-plot method. Total pore volume (V_T) was calculated from the adsorption capacity of N_2 adsorption isotherm at P/P_0 of 0.99. In addition, surface chemistry was characterized by X-ray photoelectron spectroscopy (XPS, PHI-5,300, America). The binding energy was calibrated with C1 s at 284.8 eV.

2.3 Static adsorption of VOCs on fibers

Adsorption isotherms of benzene and ethanol (A.R., Beijing Modern Eastern Finechemical Co., Ltd, China) on fibers were measured at 20 °C using a volumetric adsorption

Table 1 Conditions for carbonization and activation, burn-off, average diameter and sample ID of various fibers

Pristine PAN fiber	Carbonization	Activation	Burn-off	Average dia.	Sample ID
Electrospun from 10 wt% solution	800 °C, 30 min	800 °C, 30 min[a]	–	140 nm (90–200 nm)	ACNF10-800
Electrospun from 15 wt% solution	800 °C, 30 min	800 °C, 30 min[a]	–	650 nm (550–850 nm)	ACNF15-800
	850 °C, 30 min	850 °C, 10 min[a]	30 mass%	820 nm (590–1,010 nm)	ACNF15-850-w30
	850 °C, 30 min	850 °C, 50 min[a]	70 mass%	870 nm (700–1,040 nm)	ACNF15-850-w70
	850 °C, 30 min	850 °C, 30 min[a]	80 mass%	780 nm (480–970 nm)	ACNF15-850-w80
Meltspun	850 °C, 30 min	850 °C, 30 min[b]	–	16 μm	ACF-850

[a] by using N_2 containing 30 vol.% H_2O

[b] by using N_2 containing 50 vol.% H_2O

system (Belsorp-max, Japan). Samples (about 50 mg) were degassed for 18 h at 200 °C under 50 mL min^{-1} nitrogen flow. After pretreatment, the accurate weight of sample was measured to obtain the isotherms. The organic liquids used to generate the vapors were fully degassed by repeated evacuation before the test. System temperature was maintained by the constant temperature instrument. Saturation pressures of VOCs dependent on the temperature were calculated with the Antoine equation (Reid et al. 1986). Benzene and ethanol were selected mainly because of different dipole moment, as shown in (Table 2) (Smallwood 1996). After inputting the above parameters into testing system software, the apparatus measured the adsorption capacities at different pressures to obtain the isotherms.

3 Results

3.1 ACNFs and ACF

The typical SEM images of two ACNFs and ACF are shown in (Fig. 1). It can be seen that the diameter of ACNF is much smaller than that of ACF, and ACNF prepared by using 10 wt% PAN solution (ACNF10-800) has much smaller fiber diameter than that by 15 wt% solution (ACNF15-800). The diameter of ACNF10-800 varies from 90 to 200 nm, and the average value is about 140 nm. The average diameter of ACNF15-800 is around 650 nm, ranging from 550 to 850 nm. In case of ACF, the average diameter is 16 μm approximately.

The nitrogen adsorption/desorption isotherms of ACNFs and ACF are shown in (Fig. 2a). All the isotherms belong to type I by IUPAC classification, representing that the fibers are microporous (Brunauer et al. 1940). The three isotherms are so tightly close, indicating that the samples possess similar pore characteristics. The textural parameters of samples are summarized in (Table 3), suggesting that they have almost the same total specific surface area (S_T), micropore volume (V_m) and average pore width. The pore size distributions of samples calculated by nonlocal density functional theory (NLDFT) (Fig. 2b) reveal that micropores dominate in three kinds of fibers, which is consistent with the results of N_2 adsorption isotherms. Furthermore, the pore widths of three fibers distribute similarly and ACF has a little bit narrower pore size distribution.

Table 2 Saturation pressure, boiling point and dipole moment of benzene and ethanol

Adsorbate	Saturation pressure (kPa) at 20 °C	Boiling point (°C)	Dipole moment (D)
Benzene	10.03	80.1	0
Ethanol	5.87	78.4	1.7

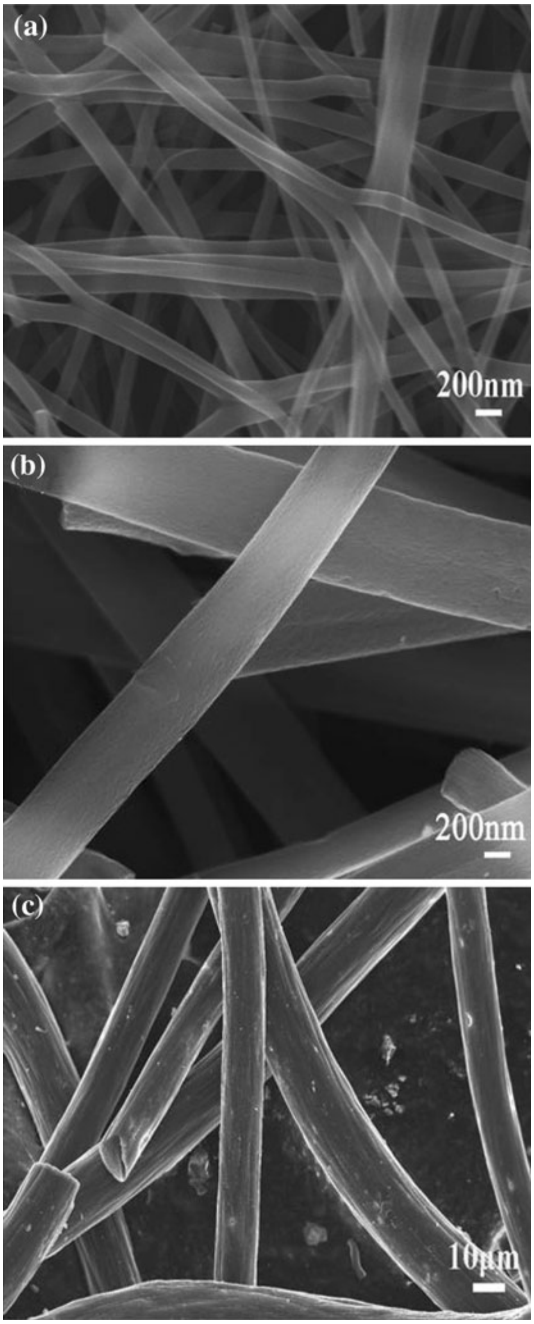

Fig. 1 SEM images of **a** ACNF10-800, **b** ACNF15-800 and **c** ACF-850

Fig. 3a shows the adsorption isotherms of benzene at 20 °C on two ACNFs and ACF. The adsorption of benzene increases sharply at low relative pressure and obvious difference in adsorption capacity among the samples can be observed at high relative pressure. In particular, the saturated adsorption amount of ACNF10-800 for benzene is 84 $\mathrm{cm}^3\ \mathrm{g}^{-1}$, while in the case of ACF-850, it is 68 $\mathrm{cm}^3\ \mathrm{g}^{-1}$.

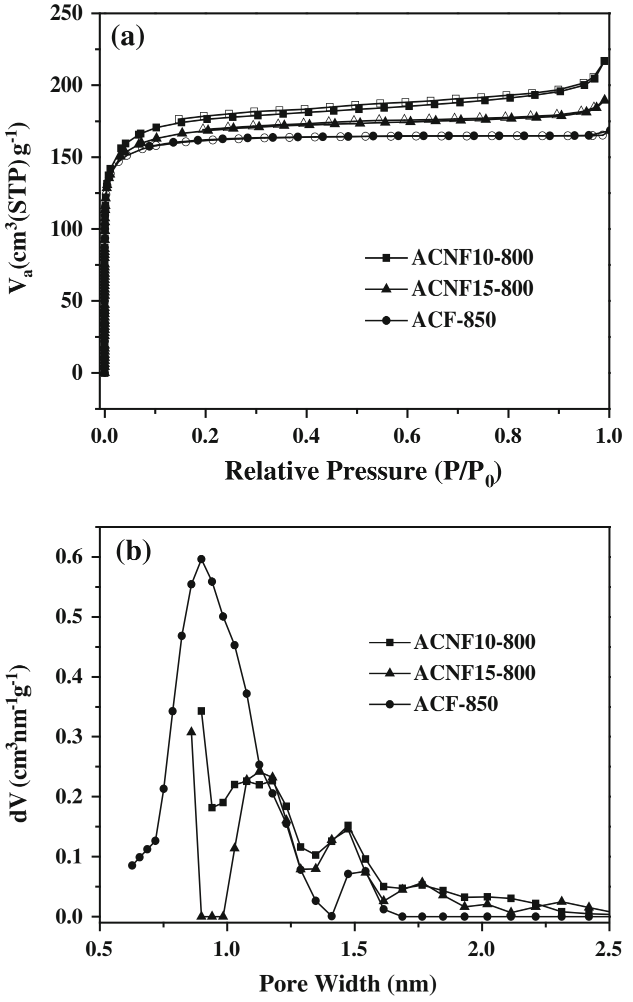

Fig. 2 **a** Nitrogen adsorption/desorption isotherms at 77 K and **b** pore size distributions of ACNF10-800, ACNF15-800 and ACF-850

It suggests that the ACNF with small diameter is a promising adsorbent for removing VOCs at high relative pressure. In order to clearly observe the difference of benzene adsorption at low relative pressures, (Fig. 3b) shows the adsorption isotherms with the relative pressure in a logarithmic form. The adsorbed amounts of benzene on two nanofibers are higher than that on the ACF at low relative pressures ($p/p_0 < 0.01$), indicating that ACNFs are more effective in adsorbing VOCs at extremely low relative pressures.

The experimental results show that ACNFs prepared via electrospinning have better performance for benzene adsorption, suggesting better performance for VOCs adsorption, even though their pore characteristics are very similar to those for ACFs prepared via meltspinning.

3.2 ACNFs with different burn-offs

In order to understand the effect of activation conditions for carbon nanofibers, PAN nanofibers prepared from 15 wt% solution were carbonized and activated at 850 °C by different conditions to give different burn-offs, denoted as ACNF15-850-w30, 70 and 80 (Table 1). It should be pointed out that ACNF15-850-w70 had a lower burn-off (70 mass%) due to an accidental decrease in steam concentration upon activation, although it was obtained at 850 °C for 50 min.

SEM images in (Fig. 4) show that the diameters of three samples are similar to each other and the average values range from 780 to 870 nm. The surface of nanofibers becomes rougher with the yield decreasing, in other words, with the burn-off increasing during activation.

Fig. 5a shows the nitrogen adsorption/desorption isotherms on three samples. All the isotherms belong to type I. Nitrogen adsorption capacity increases with the increase of the burn-off, indicating that ACNF15-850-w80 has the most developed microporous structure among the three samples. The textural parameters of the three samples are listed in (Table 3). From ACNF15-850-w30 to 80, S_T, V_T and V_m increase. The pore size distributions of nanofibers with different burn-offs (Fig. 5b) exhibit that all the three samples have multiple peaks of pore width below 2 nm, suggesting that micropore is the dominant type. ACNF15-850-w80 possesses the largest pore volume with pore widths in the range 1–2 nm among three samples, which is in agreement with its largest average pore width (Table 3).

Fig. 6 shows the C1 s signal of three samples and peaks differentiated stand for different surface oxygen groups. The peaks at 284.9, 286.2, 287.2, 288.4 eV (denoted as C1 s A, B, C and D, respectively, in (Fig. 6)) can be attributed to the C–C (graphitic), C–O (hydroxyl), C=O (carbonyl) and O = C–O bonds (carboxyl), respectively (Ryu et al. 1999), whose contents listed in Table 4 were calculated according to their atomic peak area. The O/C ratios of ACNF15-850-w70 and 80 are higher than that of ACNF15-850-w30. In addition, the O = C–O bond content decreases with the increase of the burn-off, unlike other oxygen groups.

Fig. 7 shows the adsorption/desorption isotherms for benzene and ethanol on three samples at 20 °C. It can be seen that the adsorbed amounts of benzene and ethanol at different relative pressures increase with increasing burn-off. Adsorption increases remarkably and reaches to a high value at low relative pressure below 0.1. At the highest relative pressure, the benzene adsorption capacities of ACNF15-850-w30, 70 and 80 are 53, 57 and 104 cm^3 g^{-1}, and in case of ethanol the values are 84, 117, and 135 cm^3 g^{-1}, respectively. Thus ACNF15-850-w80 has the best adsorption performance among the three samples. Additionally, for benzene and ethanol, two VOC molecules with different properties, the adsorption performance of ACNFs is different as shown clearly in (Fig. 7c).

Table 3 Textural parameters of various fibers

Sample ID	S_T ($m^2\ g^{-1}$)	V_T ($cm^3\ g^{-1}$)	V_m ($cm^3\ g^{-1}$)	APW (nm)
ACNF10-800	791	0.33	0.27	0.68
ACNF15-800	771	0.29	0.26	0.67
ACF-850	770	0.26	0.25	0.65
ACNF15-850-w30	581	0.23	0.20	0.69
ACNF15-850-w70	667	0.27	0.24	0.72
ACNF15-850-w80	931	0.38	0.34	0.73

S_T total specific surface area, V_T total pore volume, V_m micropore volume, *APW* average pore width

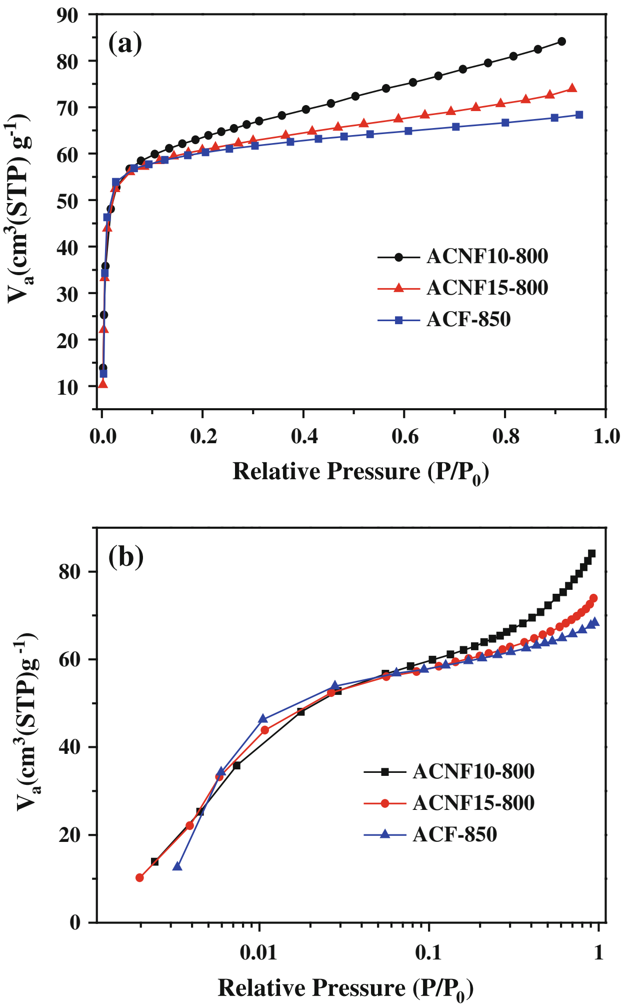

Fig. 3 **a** Adsorption isotherms of benzene on three samples at 20 °C and **b** adsorption isotherms with the relative pressure in a logarithmic form

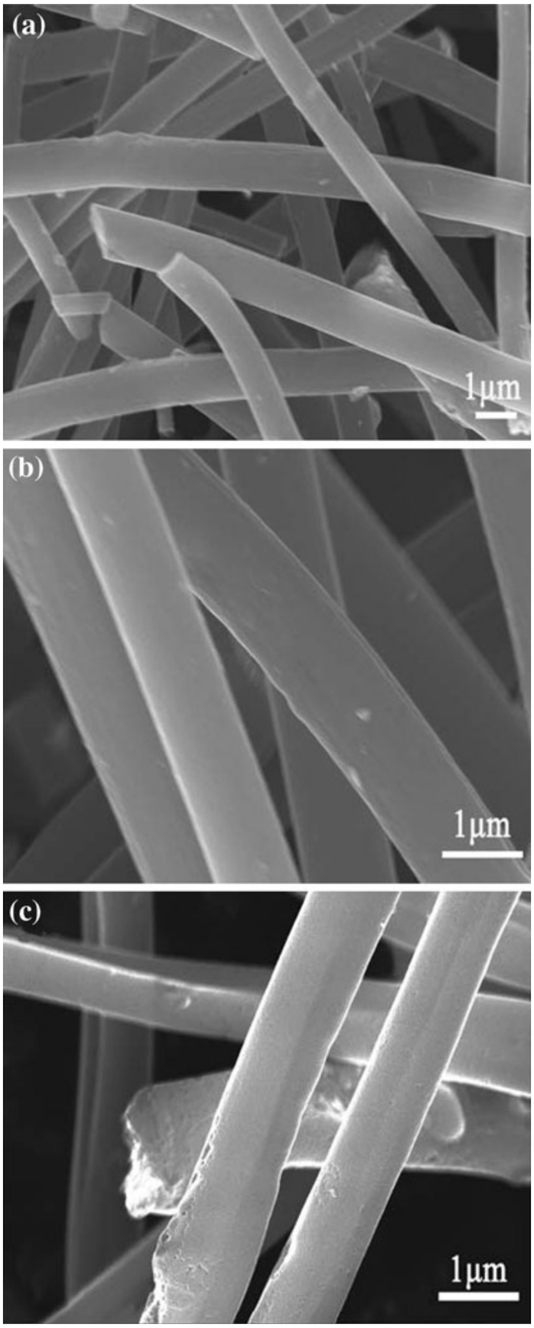

Fig. 4 SEM images of **a** ACNF15-850-w30, **b** ACNF15-850-w70 and **c** ACNF15-850-w80

4 Discussion

4.1 Adsorption characteristics of fibrous carbon with different diameters

Since ACNF10-800, ACNF15-800 and ACF-850 are porous fibers dominated by micropores (Fig. 2; Table 3), high

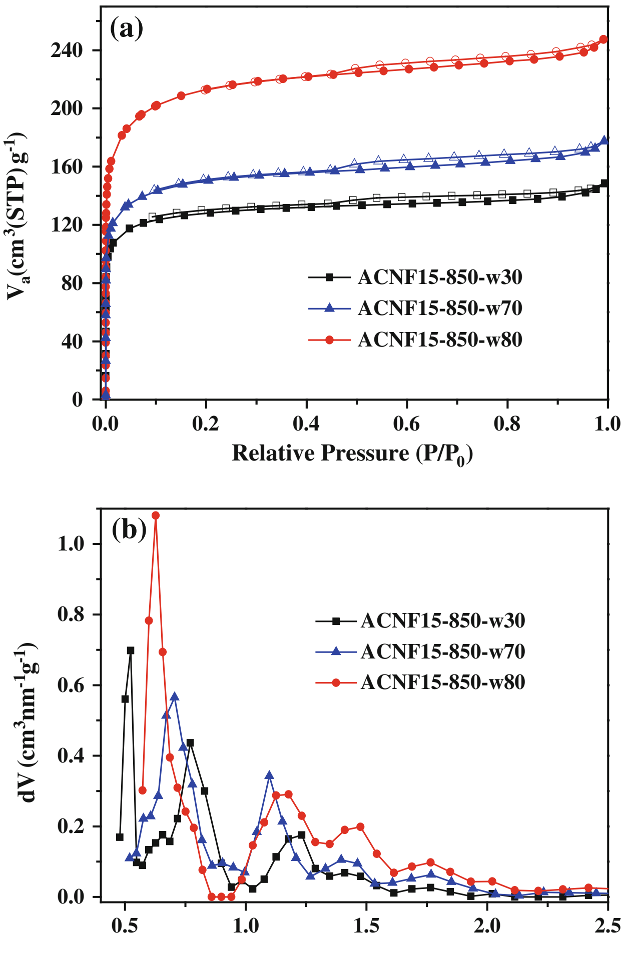

Fig. 5 **a** Nitrogen adsorption/desorption isotherms at 77 K and **b** pore size distributions of ACNF15-850-w30, 70 and 80

adsorption amounts of three samples for benzene at low relative pressures correspond that micropores provide most of adsorption sites and form strong interaction with adsorbate molecule (Hsieh and Chen 2007). The similar micropore volume of three samples results in almost the same adsorption amounts at the knee of isotherms.

The variation in adsorption performance for VOCs on two ACNFs and ACF could be attributed to the remarkably different fiber diameters (Fig. 1), since they have similar pore characteristics and total specific surface area (Fig. 2; Table 3). As ACNFs have much smaller diameter than ACF, micropores on the surface of ACNFs would be more shallow and homogenous, and if not, the surface area would not be similar, considering that the external surface area per unit weight of ACNF should be larger than that of the thick ACF (Lee et al. 2010, 2006). In this case, VOC molecules could reach the adsorption sites more easily and quickly from pore entrance. In addition, micropores could

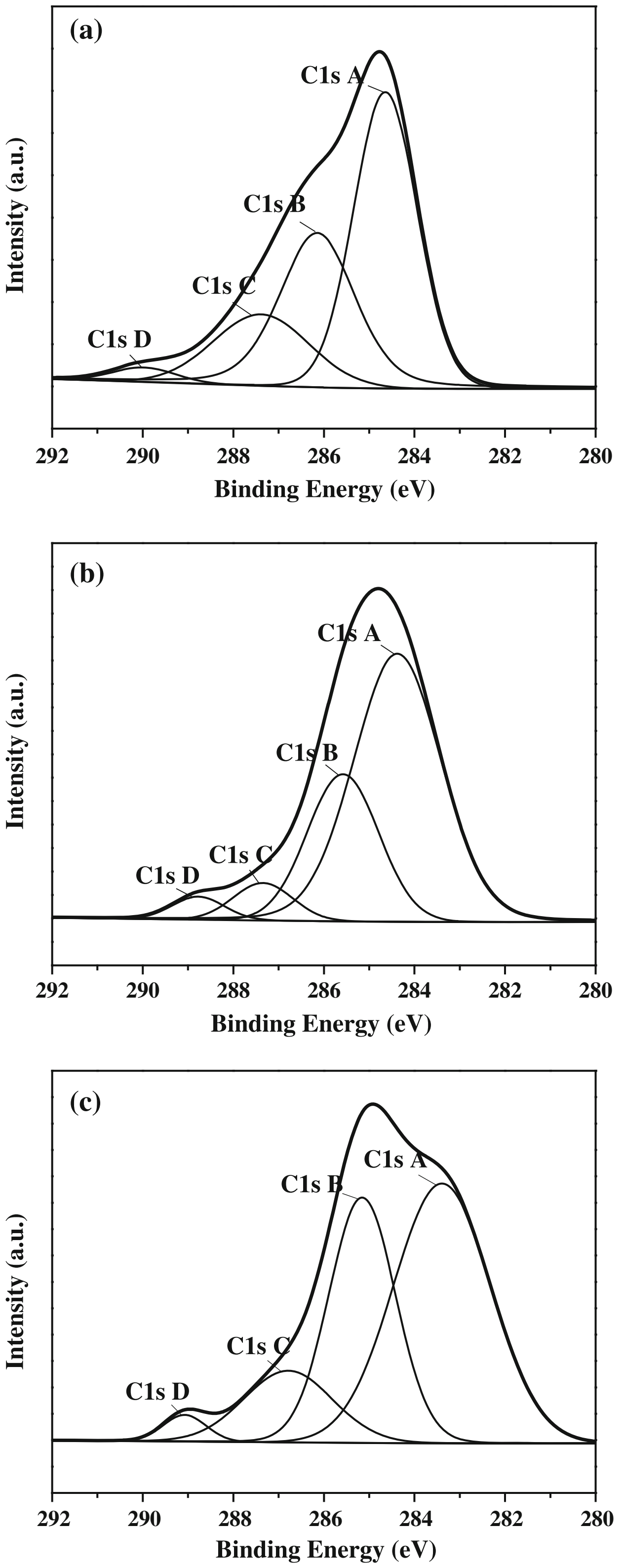

Fig. 6 XPS C1 s signal of **a** ACNF15-850-w30, **b** ACNF15-850-w70 and **c** ACNF15-850-w80

Table 4 Surface composition characterized by XPS

Sample ID	C (at.%)	O (at.%)	O/C	C–O (at.%)	C=O (at.%)	O = C–O (at.%)
ACNF15-850-w30	85.8	11.3	0.13	17.9	8.0	1.05
ACNF15-850-w70	80.6	17.2	0.21	29.2	4.0	0.60
ACNF15-850-w80	82.6	15.2	0.18	23.8	7.3	0.32

not be occupied entirely by adsorbate molecules at low relative pressures (Lillo-Ródenas et al. 2006), indicating that the adsorption sites could not be utilized entirely during adsorption process. It should be noted that, for the same mass of ACNFs and ACFs, the amount of shallow pores is higher than that of deep pores, which means that ACNFs can supply more available adsorption sites for VOC molecules at low relative pressures. As a result, more benzene molecules are adsorbed onto ACNF10-800 and ACNF15-800 at low relative pressures, resulting in the higher adsorption amount of nanofibers than that of ACF-850.

4.2 Adsorption characteristics of ACNFs with different burn-offs

Different activation conditions have obvious effects on the physical and chemical properties of ACNFs. (Fig. 7) shows that the adsorption performance of ACNFs becomes better with the increase of the burn-off during activation. The adsorption performance is consistent with the fact that more developed microporosity forms in nanofibers with increasing burn-off. The porous structure of ACNFs is a key point dominating adsorption properties. Larger total specific surface area and micropore volume (S_T and V_T) can result in higher adsorption capacities of VOCs. Therefore, ACNF15-850-w80 can be concluded as a more effective adsorbent for benzene and ethanol than ACNF15-850-w30 and w70.

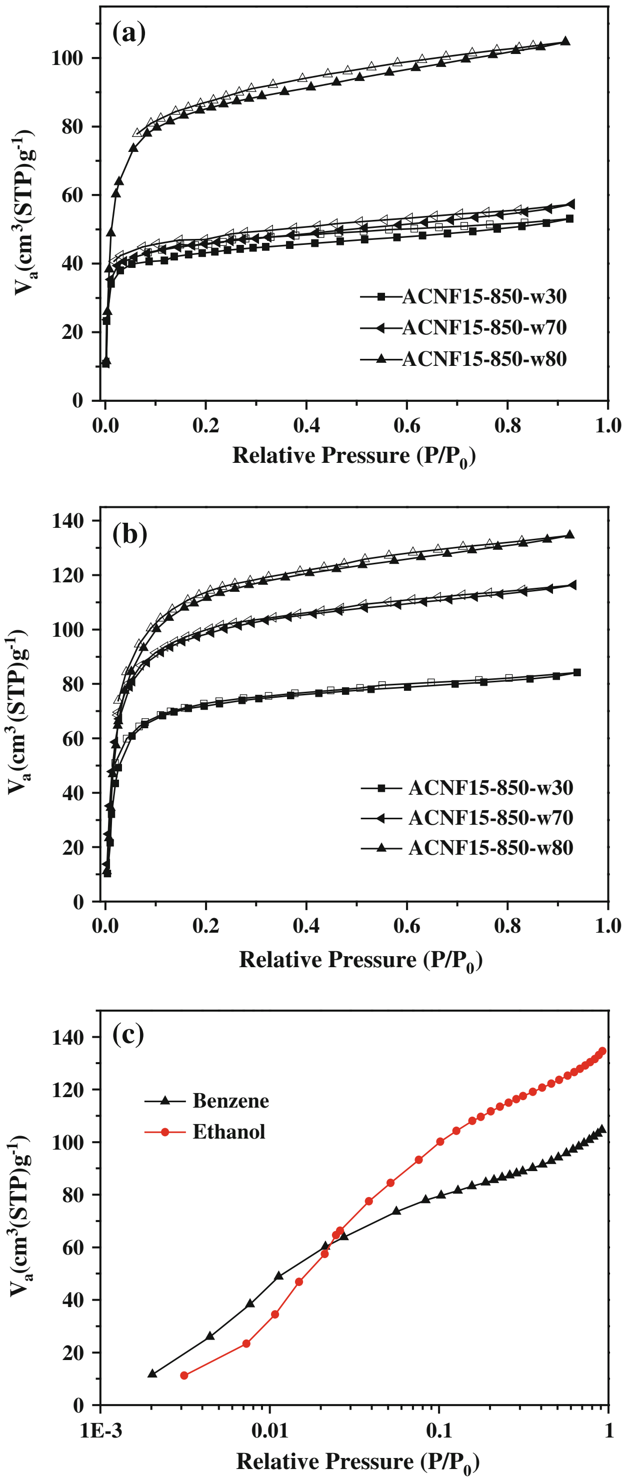

Fig. 7 Adsorption/desorption isotherms of **a** benzene and **b** ethanol on three samples, and **c** adsorption isotherms of benzene and ethanol on ACNF15-850-w80 at 20 °C

Besides, surface chemistry is another factor influencing the adsorption performance. The π–π interaction between the π electron rich region on carbon surface and the aromatic ring can promote the adsorption of aromatic hydrocarbon (Garcia et al. 2004; Tsai et al. 2008). Surface oxygen groups could restrict this interaction and weaken the adsorption of benzene (non-polarity). Thus, ACNF15-850-w70 with the highest oxygen content exhibits a close adsorption capacity of benzene with ACNF15-850-w30. Cuervo et al. (2008) described that carbon nanofibers after oxidation had more carboxyl and anhydride on the surface, resulting in lower adsorption capacities for benzene and toluene. The lowest content of carboxyl groups on the surface of ACNF15-850-w80 among three samples may contribute to the best adsorption performance of benzene on ACNF15-850-w80. In addition, higher O/C ratio on ACNFs, indicating a higher polarity of surface, can promote the adsorption of polar VOC molecules (Tsai et al. 2008). Since all of ACNFs with high O/C ratio larger than 0.1 exhibit the polar surface, the adsorption capacity of ethanol is higher than that of benzene. Especially, due to the highest O/C ratio, ACNF15-850-w70 possesses the most significantly improved adsorption for ethanol.

It should be noted that the adsorption amount of ethanol on ACNF15-850-w80 is larger than that of benzene over most of the relative pressures (P/P_0 larger than 0.03). However, the inverse fact can be seen clearly that its adsorption value of benzene is higher than that of ethanol at low relative pressures ($p/p_0 < 0.03$) in (Fig. 7c). The higher adsorption value of benzene at extremely low relative pressures could be attributed to the different molecule structure of benzene and ethanol. The adsorption affinity is dependent on the micropore structure at low relative pressures (Ramos et al. 2010). Benzene with a disc-like structure could go through the narrow constrictions in pore entrances more easily to arrive at the adsorption sites (Brasquet and Le Cloirec 1999; Liu et al. 2008). Meanwhile, for non-polar compounds such as benzene, physical properties play more important roles than surface chemistry at low relative pressures (Tsai et al. 2008). Thus, adsorption behavior of benzene at extremely low relative pressures can be enhanced.

According to the above discussion, the factors contributing to the mechanism of VOCs adsorption are related to the properties of both adsorbent and adsorbate. The developed microporous structure of fibers plays a key role during the adsorption process. Besides, surface functional groups of ACNFs, structure and polarity of VOC adsorbates could also have obvious effects on the adsorption performance.

5 Conclusion

ACNFs were fabricated by the method of electrospinning and steam activation. Due to the much smaller fiber diameter, micropores on the surface of ACNFs are supposed to be shallower and available adsorption sites would be more. As a result, ACNFs demonstrate higher adsorption capacities for VOCs than ACF at extremely low relative pressures. When the nanofibers were activated by different conditions, the microporosity of ACNFs increased with increasing burn-off. The higher total specific surface area and micropore volume can result in higher adsorption capacities of benzene and ethanol at different relative pressures. In addition, surface chemistry has an important effect on the adsorption of polar VOCs. The ACNF with higher oxygen content possesses a higher adsorption capacity for ethanol.

Activation condition for carbon nanofibers having nanometer-size diameters is reasonably supposed to be different from that for carbon fibers having much larger diameters (micrometer size). Therefore, more detailed researches are required to optimize the activation condition for nanofibers for the development of effective adsorbent for VOCs removal.

Acknowledgments The authors acknowledge the financial support of the cooperative project JST-MOST (No. 2011DFA50430), the national high technology research and development program of China (863 Program-No. 2010AA064907) and the program for new century excellent talents in university (NCET-10-0496).

References

Benkhedda, J., Jaubert, J.N., Barth, D., Perrin, L.: Experimental and modeled results describing the adsorption of toluene onto activated carbon. J. Chem. Eng. Data **45**(4), 650–653 (2000)

Brasquet, C., Le Cloirec, P.: Effects of activated carbon cloth surface on organic adsorption in aqueous solutions. Use of statistical methods to describe mechanisms. Langmuir **15**(18), 5906–5912 (1999)

Brunauer, S., Deming, L.S., Deming, W.E., Teller, E.: On a theory of the van der waals adsorption of gases. J. Am. Chem. Soc. **62**, 1723–1732 (1940)

Chen, W., Duan, L., Zhu, D.Q.: Adsorption of polar and nonpolar organic chemicals to carbon nanotubes. Environ. Sci. Technol. **41**(24), 8295–8300 (2007)

Cuervo, M.R., Asedegbega-Nieto, E., Diaz, E., Vega, A., Ordonez, S., Castillejos-Lopez, E., Rodriguez-Ramos, I.: Effect of carbon nanofiber functionalization on the adsorption properties of volatile organic compounds. J. Chromatogr. A **1188**(2), 264–273 (2008)

Dolidovich, A.F., Akhremkova, G.S., Efremtsev, V.S.: Novel technologies of VOC decontamination in fixed, moving and fluidized catalyst-adsorbent beds. Can. J. Chem. Eng. **77**(2), 342–355 (1999)

Dwivedi, P., Gaur, V., Sharma, A., Verma, N.: Comparative study of removal of volatile organic compounds by cryogenic condensation and adsorption by activated carbon fiber. Sep. Purif. Technol. **39**(1–2), 23–37 (2004)

Garcia, T., Murillo, R., Cazorla-Amoros, D., Mastral, A.M., Linares-Solano, A.: Role of the activated carbon surface chemistry in the adsorption of phenanthrene. Carbon **42**(8–9), 1683–1689 (2004)

Hsieh, C.T., Chen, W.Y.: Gaseous adsorption of carbon tetrachloride onto carbon nanofiber arrays prepared by template-assisted synthesis. Diamond Relat. Mater. **16**(11), 1945–1949 (2007)

Hsieh, C.T., Chou, Y.W.: Fabrication and vapor-phase adsorption characterization of acetone and n-hexane onto carbon nanofibers. Sep. Sci. Technol. **41**(14), 3155–3168 (2006)

Jahangiri, M., Shahtaheri, S.J., Adl, J., Rashidi, A., Kakooei, H., Forushani, A.R., Ganjali, M.R., Ghorbanali, A.: The adsorption of benzene, toluene and xylenes (BTX) on the carbon nanostructures: the study of different parameters. Fresenius Environ. Bull. **20**(4A), 1036–1045 (2011)

Tsai, J.-H., Chiang, H.-M., Huang, G.-Y., Chiang, H.-L.: Adsorption characteristics of acetone, chloroform and acetonitrile on sludge-derived adsorbent, commercial granular activated carbon and activated carbon fibers. J. Hazard. Mater. **15**(1–3), 1183–1191 (2008)

Lee, K.J., Shiratori, N., Lee, G.H., Miyawaki, J., Mochida, I., Yoon, S.-H., Jang, J.: Activated carbon nanofiber produced from electrospun polyacrylonitrile nanofiber as a highly efficient formaldehyde adsorbent. Carbon **48**(15), 4248–4255 (2010)

Lillo-Ródenas, M.A., Cazorla-Amorós, D., Linares-Solano, A.: Behaviour of activated carbons with different pore size distributions and surface oxygen groups for benzene and toluene adsorption at low concentrations. Carbon **43**(8), 1758–1767 (2005)

Lillo-Ródenas, M.A., Fletcher, A.J., Thomas, K.M., Cazorla-Amorós, D., Linares-Solano, A.: Competitive adsorption of a benzene-toluene mixture on activated carbons at low concentration. Carbon **44**(8), 1455–1463 (2006)

Liu, C.H., Li, J.J., Zhang, H.L., Li, B.R., Guo, Y.: Structure dependent interaction between organic dyes and carbon nanotubes. Coll. Surf. **313**, 9–12 (2008)

Oh, G.Y., Ju, Y.W., Jung, H.R., Lee, W.J.: Preparation of the novel manganese-embedded PAN-based activated carbon nanofibers by electrospinning and their toluene adsorption. J. Anal. Appl. Pyrolysis **81**(2), 211–217 (2008a)

Oh, G.Y., Ju, Y.W., Kim, M.Y., Jung, H.R., Kim, H.J., Lee, W.J.: Adsorption of toluene on carbon nanofibers prepared by electrospinning. Sci. Total Environ. **393**(2–3), 341–347 (2008b)

Ramos, M.E., Bonelli, P.R., Cukierman, A.L., Carrott, M., Carrott, P.J.M.: Adsorption of volatile organic compounds onto activated carbon cloths derived from a novel regenerated cellulosic precursor. J. Hazard Mater. **177**(1–3), 175–182 (2010)

Reid, R.C., Prausnitz, J.M., Poling, B.E.: The properties of gases and liquids. McGraw Hill, New York (1986)

Ryu, S.-K., Park, B.-J., Park, S.-J.: XPS analysis of carbon fiber surfaces–anodized and interfacial effects in fiber-epoxy composites. J. Coll. Interface Sci. **215**(1), 167–169 (1999)

Shim, W.G., Kim, C., Lee, J.W., Yun, J.J., Jeong, Y.I., Moon, H., Yang, K.S.: Adsorption characteristics of benzene on electrospun-derived porous carbon nanofibers. J. Appl. Polym. Sci. **102**(3), 2454–2462 (2006)

Smallwood, I.M.: Handbook of arganic solvent properties. Halsted Press, New York (1996)

Tavanai, H., Jalili, R., Morshed, M.: Effects of fiber diameter and CO2 activation temperature on the pore characteristics of polyacrylonitrile based activated carbon nanofibers. Surf. Interface Anal. **41**(10), 814–819 (2009)

Wang, M.-X., Huang, Z.-H., Kang, F., Liang, K.: Porous carbon nanofibers with narrow pore size distribution from electrospun phenolic resins. Mater. Lett. **65**(12), 1875–1877 (2011a)

Wang, M.-X., Huang, Z.-H., Shimohara, T., Kang, F., Liang, K.: NO removal by electrospun porous carbon nanofibers at room temperature. Chem. Eng. J. **170**(2-3), 505–511 (2011b)

Yi, F.Y., Lin, X.D., Chen, S.X., Wei, X.Q.: Adsorption of VOC on modified activated carbon fiber. J. Porous Mater. **16**(5), 521–526 (2009)